Limnol. Oceanogr., 50(1), 2005, 311–327

Particle export during the Southern Ocean Iron Experiment (SOFeX)

K. O. Buesseler, J. E. Andrews, S. M. Pike, and M. A. Charette
Department of Marine Chemistry and Geochemistry, Woods Hole Oceanographic Institution, Woods Hole, Massachusetts 02543

L. E. Goldson[1]
University of East Anglia, Norwich, Norfolk NR4 7TJ, Great Britain

M. A. Brzezinski
Department of Ecology Evolution and Marine Biology and the Marine Science Institute, University of California, Santa Barbara, California 93106

V. P. Lance
Duke University, Nicholas School of the Environment and Earth Sciences, Beaufort, North Carolina 28516

Abstract

We studied the effect of iron addition on particle export in the Southern Ocean by measuring changes in the distribution of thorium-234 during a 4-week iron (Fe) enrichment experiment conducted in the high-silicate high-nitrate waters just south of the Southern Antarctic Circumpolar Current Front at 172.5°W. Decreases in ^{234}Th activity with time in the fertilized mixed layer (0–50 m) exceeded those in unfertilized waters, indicating enhanced export of ^{234}Th on sinking particles after Fe enrichment. The addition of Fe also affected export below the fertilized patch by increasing the efficiency of particle export through the 100-m depth horizon. Extensive temporal and vertical Lagrangian sampling allowed us to make a detailed examination of the ^{234}Th flux model, which was used to quantify the fluxes of particulate organic carbon (POC) and biogenic silica ($bSiO_2$). Iron addition increased the flux of both POC and $bSiO_2$ out of the mixed layer by about 300%. The flux at 100 m increased by more than 700% and 600% for POC and $bSiO_2$, respectively. The absolute magnitude of the POC and $bSiO_2$ fluxes were not large relative to natural blooms at these latitudes or to those found in association with the termination of blooms in other ocean regions. Our results support the hypothesis that Fe addition leads directly to significant particle export and sequestration of C in the deep ocean. This is a key link between ocean Fe inputs and past changes in atmospheric CO_2 and climate.

The ''iron hypothesis'' (Martin 1990), suggests that inputs of the limiting micronutrient, iron, in high-nutrient low-chlorophyll (HNLC) regions results in enhanced growth of marine phytoplankton. This hypothesis has now been validated in many HNLC regions, including the Southern Ocean (Coale et al. 1996; Boyd et al. 2000). However, it has been difficult to quantify whether or not this growth response results in enhanced export of sinking particulate organic carbon to the deep ocean. Increased new production and carbon export is the primary mechanism by which either natural or anthropogenic iron enrichments could sequester carbon in the deep ocean and thus affect climate. The Southern Ocean is of particular interest in this regard because productivity in this region has been shown to be iron (Fe) limited (Boyd et al. 1999; Smetacek 2001; Coale et al. 2004), and surface waters return to depth with high levels of macronutrients that could be used by phytoplankton if Fe supply were higher.

The Southern Ocean Iron Experiment (SOFeX) was a deliberate iron enrichment study that involved three research vessels and a large group of scientists studying the biogeochemical response of the surface ocean to iron at two sites: one north of the Polar Frontal zone in the low-silicate waters of the sub-Antarctic ($Si[OH]_4 < 3$ μmol L^{-1}) and one farther south in the permanently high silicate waters to the south of the Southern Antarctic Circumpolar Current Front ($Si[OH]_4 \approx 60$ μmol L^{-1}; Coale et al. 2004). Prior studies in the Southern Ocean resulted in a diatom growth response after iron addition to moderately high silicate waters (Boyd et al. 2000). A particularly significant finding of SOFeX was the enhanced growth of a mixed community of larger cells (>5 μm diameter), including diatoms of the genus *Pseudonitz-*

[1] Present address: Plymouth Marine Laboratory, Plymouth PL1 3DH, Great Britain.

Acknowledgments

SOFeX involved many collaborators, without whom this study would not have been possible. In particular, we thank K. Coale, K. Johnson, and the scientists and crews aboard the RV *Revelle*, RV *Melville*, and U.S. Coast Guard RIB *Polar Star* for their help and assistance. We could also not have written this paper without the open sharing of SOFeX data produced by other investigators that are discussed here or used in the figures; in this regard, we particularly thank E. Abraham, R. Barber, R. Wanninkhof, and F. Chavez. This article benefited from comments by R. Anderson and an anonymous reviewer. This work was supported by the Division of Ocean Sciences at the U.S. National Science Foundation, the Biological and Environmental Research Office, Office of Science, U.S. Department of Energy, and for RIB Polar Star logistical support, Polar Programs at the U.S. National Science Foundation.

schia, dinoflagellates, and the prymnesiophyte *Phaeocystis,* in the low-silicate ''North Patch.'' The growth response differed in the high-silicate ''South Patch,'' where up to 65% of the phytoplankton in the bloom were diatoms (M. Landry pers. comm.). A complete overview of both experiments and the primary growth and geochemical responses can be found in Coale et al. (2004).

Here we use the naturally occurring radionuclide thorium-234 ($t_{½}$ = 24.1 d) as an in situ tracer of particle flux during SOFeX. In this manuscript, we focus on results from the South Patch and examine the details of the changes in particle export as a response to iron. North Patch ^{234}Th data were too limited (n = 2 occupations) to make any conclusions regarding changes in particle export. Newly developed improvements in ^{234}Th analytical protocols (Buesseler et al. 2001*a*) and a coordinated effort between two ships over a 4-week period resulted in one of the most extensive sets of ^{234}Th data ever collected. A brief overview of these results has been presented previously (Buesseler et al. 2004), but herein we expand on these results with a detailed analyses of the time series evolution of the ^{234}Th response in the context of larger biogeochemical data sets and in terms of the ^{234}Th flux model, its uncertainties, and its application to the quantification of the fluxes of particulate organic carbon (POC) and other major bioelements (biogenic silica [$bSiO_2$] and particulate organic nitrogen [PON]). We also compare these data to prior observations of natural blooms at the SOFeX site and examine the export fluxes of C and Si relative to uptake rates. Finally, the particle flux response in prior Southern Ocean fertilization studies will be discussed.

Sampling and analyses

Study site and sampling protocols—Sampling took place over a 4-week period during occupation of the SOFeX South Patch in the vicinity of 66°S, 172.5°W. Four separate iron enrichments of a single patch of water were made over a grid that was initially 15 × 15 km with the use of methods described previously (Coale et al. 1998). In total, 1.26×10^3 kg of ferrous iron (as $FeSO_4$) was added to surface waters (t_0 = 0730 h GMT, 24 January 2002), resulting in Fe concentrations within the mixed layer that were expected to stimulate phytoplankton growth (~0.7 nmol L^{-1} Fe after addition). During the initial release, the inert tracer SF_6 (sulfur hexafluoride) was concomitantly added with the iron to mark the fertilized patch and to provide a Lagrangian framework for the experiment (Watson et al. 1991). We use the convention that time zero was the starting time of the initial Fe and SF_6 release, although these additions took more than 24 h to complete.

Thorium-234 samples were collected between 30 January and 14 February 2002 on the RV *Melville* (t = day 5.8–21.6) followed by the U.S. Coast Guard RIB *Polar Star* between 15 and 20 February (t = day 21.7–27.4). During each cruise, samples were collected both inside the iron-fertilized patch (hereafter referred to as IN) and at control stations outside the patch (hereafter referred to as OUT). The presence of high SF_6 at a given station was used to differentiate between IN and OUT stations.

Profiles of total ^{234}Th were collected from 4-liter samples taken from Go-Flow® or Niskin bottles deployed by rosette or as single bottles strung on Kevlar line within the upper 100–150 m on 18 separate casts. On the RV *Melville,* ^{234}Th sampling was conducted primarily with the use of a trace metal (TM) clean rosette used for primary production and other biological rate measurements and studies. SF_6 was not measured on every TM rosette cast, although SF_6 was used to identify IN versus OUT stations on at least selected surface samples at the same station. On the RIB *Polar Star,* SF_6 was measured on every cast for which ^{234}Th samples were collected.

Samples for particulate ^{234}Th, POC, and $bSiO_2$ were collected with paired battery-powered, large-volume, in situ pumps (McLane Labs) deployed to predetermined depths, usually one within (typically ~20 m) and one below the mixed layer (~50–120 m; n = 21 pump casts). Sample volumes on the order of 400 liters (measured at the outlet via an in-line mechanical flowmeter) were passed sequentially through 142-mm-diameter filters mounted in a polyvinyl chloride, baffled filter housing at flow rates of 8 L min^{-1}. The first filter was a polyester screen with a nominal mesh size of 54 μm. This was followed by a quartz filter (QMA) with a 1-μm nominal pore size.

Shallow samples were also collected along several transects from depths of either 25 m or at the surface. Surface samples for ^{234}Th, SF_6, and chlorophyll *a* (Chl *a*) were collected from the ship's uncontaminated surface seawater line or a bucket. At selected transect stations, 25-m samples were collected with either a Niskin bottle or a TM rosette.

^{234}Th analyses—Within 1 h of collection, unfiltered 4-liter samples for total ^{234}Th determination were acidified to pH 2 with 6 ml of concentrated HNO_3. After shaking the samples vigorously, 0.3 ng of ^{230}Th was added as a yield monitor. The sample was shaken again and allowed to equilibrate for 12 h. After equilibration, the pH was adjusted to 8 ± 0.15 with concentrated NH_4OH. Extraction of thorium from the samples was accomplished by coprecipitation of thorium via formation of MnO_2 precipitate formed by the addition of $KMnO_4$ and $MnCl_2$ solutions at pH 8 (Benitez-Nelson et al. 2001; Buesseler et al. 2001*a*). Samples were shaken vigorously after the addition of each reagent and after the formation of the MnO_2 precipitate, allowed to stand for 12 h followed by filtration onto 25-mm-diameter QMA filters. Finally, the filtered manganese (Mn) precipitates were dried overnight and mounted under one layer of Mylar film and two layers of standard aluminum foil in preparation for beta counting.

Particles collected on the 54-μm pore size screens were rinsed immediately after collection onto single 25-mm-diameter silver (Ag) filters (Sterlitech Corp., 1.2 μm nominal pore size) with the use of prefiltered deep water. The Ag filters were dried overnight at 60°C and prepared for beta counting with Mylar and aluminum covers identical to the ^{234}Th samples. The 142-mm-diameter QMA filters were dried overnight, and 25-mm-diameter punches (n = 20; equivalent to 52% of the active filter area) were cut, stacked, and pressed into inverted beta mounts and prepared for counting.

Analyses of particulate and total ^{234}Th activities were performed at sea with gas-flow proportional beta counters manufactured by Risø National Laboratories following methods described in Buesseler et al. (2001*a*). Initial at-sea beta counting for 6–24 h was followed by a final background count in the lab after decay of ^{234}Th for at least six half-lives. Initial count rates were typically 2–4 counts per minute (cpm) for total ^{234}Th and final count rates averaged 0.5 cpm relative to the detector backgrounds of 0.15–0.20 cpm. For total ^{234}Th samples, anion exchange chemistry was performed, and recovery of our added ^{230}Th yield monitor was quantified by inductively coupled plasma–mass spectroscopy with addition of a ^{229}Th internal standard (Pike et al. in press). Corrections were applied to ^{234}Th activity calculations on the basis of ^{230}Th recoveries. All data are decay corrected to the time of collection and reported with a propagated error that includes uncertainty associated with counting, sample volumes, and other calibration errors. Errors were typically $\pm$0.04–0.06 dpm L^{-1} on total ^{234}Th.

A recommended check on overall accuracy of the total ^{234}Th activity measurement is through analyses of deep waters in which equilibrium with ^{238}U is assured (i.e., ^{234}Th = ^{238}U, with ^{238}U being derived from salinity; Chen et al. 1986). On the RV *Melville,* we analyzed eight samples from 1,400 m and found a 3.0% standard deviation in ^{234}Th activity. On the RIB *Polar Star,* we were only able to collect two 4-liter samples from 500 m, and the ^{234}Th activities were identical to ^{238}U within our error of $\pm$2%. Having made this calibration, one can be certain that the ^{234}Th : ^{238}U ratio in the surface accurately reflects the ^{234}Th : ^{238}U disequilibrium that is used to calculate the fluxes that are central to the application of this tracer.

POC, PON, and $bSiO_2$—All samples for POC, PON, and $bSiO_2$ analyses were taken from the same filter matrix that had been analyzed for ^{234}Th, enabling the particulate ratio of each element to ^{234}Th to be determined. Thus, the >54-μm particles, which had been rinsed onto 25-mm-diameter Ag filters and counted for ^{234}Th, were subsequently subsampled by weight for POC, PON, and $bSiO_2$ analyses. Subsamples of the QMA filter were obtained by removing a small punch from the 142-mm-diameter filter and analyzing by standard methods for POC and PON. Prior to CHN (carbon, hydrogen, nitrogen) analyses, all samples were fumed with HCl to remove carbonate (Pike and Moran 1997). CHN analyses were performed with a Thermo Quest Flash EA 1112 (CE Instruments). Biogenic silica was not measured on the QMA fraction because of the high Si blanks associated with this filter matrix (Buesseler et al. 2001*a*). Details of the NaOH digestion methods and analyses used to determine $bSiO_2$ on Ag filters are described in Brzezinski et al. (2001) and Buesseler et al. (2001*b*).

Chlorophyll and primary production—For the SOFeX South Patch, chlorophyll and primary productivity were measured from patch days of ca. -1.5 to $\sim$19.5 (from aboard the RV *Roger Revelle*: $t = -1.5$ to 9.5 and aboard the RV *Melville*: $t = \sim 7$ to 19.5). Surface chlorophyll was measured aboard the RIB *Polar Star* for patch days $\sim$21.5 to 27.5. Selections of these chlorophyll and productivity data have been presented in Coale et al. (2004), and methods are only summarized here. Chl *a* samples were collected from a standard rosette (or shipboard underway system in the case of *Polar Star*), filtered onto Whatman (GF/F) glass fiber filters, extracted with 90% acetone for 24 h in the dark at -20°C (Venrick and Hayward 1984), and analyzed fluorometrically (Holm-Hansen et al. 1965; Lorenzen 1966). Primary productivity samples were collected from the trace metal–clean rosette (Hunter et al. 1996), with the use of clean techniques to minimize trace metal contamination, and incubated on deck (Barber et al. 1996). Water samples were collected into 75-ml sterile polycarbonate tissue culture flasks, inoculated with 10 μCi of ^{14}C-carbonate solution, and incubated for 24 h in incubators screened with blue plastic plus neutral-density screening to achieve a given percentage of surface incident irradiance ($E_d[0^-]$)—nominally 100%, 47%, 16%, 10%, and 1%. Incubator temperatures were maintained by a continuous flow of surface seawater. Incubated samples were harvested on Whatman (GF/F) filters and acidified with 0.5 ml of 0.5 N HCl for 24 h, scintillation was fluid added, and, after another 24 h in the dark at room temperature, sample activities were counted in a liquid scintillation counter. Time zero controls and total added activity were determined similarly by variations on the methods described in "^{234}*Th analyses*" (Huntsman and Barber 1977).

Results

Transect data—The main objective of this study was to determine whether an Fe-induced increase in plankton biomass also leads to an increase in particle export flux, as evidenced by decreased ^{234}Th activities. As a means of providing a rapid assessment of these effects, we conducted a series of surface transects across the Fe-fertilized patch. During each transect, the boundaries of the patch were clearly identifiable by the SF_6 data, which increased from background to maximum SF_6 concentrations at the patch center (background surface SF_6 levels OUT are $\sim$1–2 fmol L^{-1} because of global releases; Fig. 1). Note that the maximum SF_6 concentration along each transect decreases over time from $\sim$40 to 5 fmol L^{-1} because of dilution from horizontal patch dispersal, mixed-layer deepening, and losses across the air–sea interface (Goldson 2004). Recall that SF_6 was only added with the first of four iron additions. Although every effort was made to overlay each Fe addition within the region tagged with SF_6, some enrichment of waters without SF_6 likely occurred.

Chl *a* concentrations increased over time within the fertilized patch, providing first-order evidence that iron addition to these waters stimulated phytoplankton production, as discussed in Coale et al. (2004). However, also note in the satellite image from day 23 (Fig. 2; only clear satellite image during SOFeX) and on the transect data from days 25 and 28 (Fig. 1E,F) that high chlorophyll concentrations were also observed in unfertilized waters surrounding the patch. For example, on day 25, the transect (Fig. 1E) showed a general trend toward slightly higher ^{234}Th activities on its northern end between 65.3°S and 65.5°S. Chl *a* concentrations were $\sim$1.5 mg m^{-3} compared with a maximum of $\sim$2 mg m^{-3} at

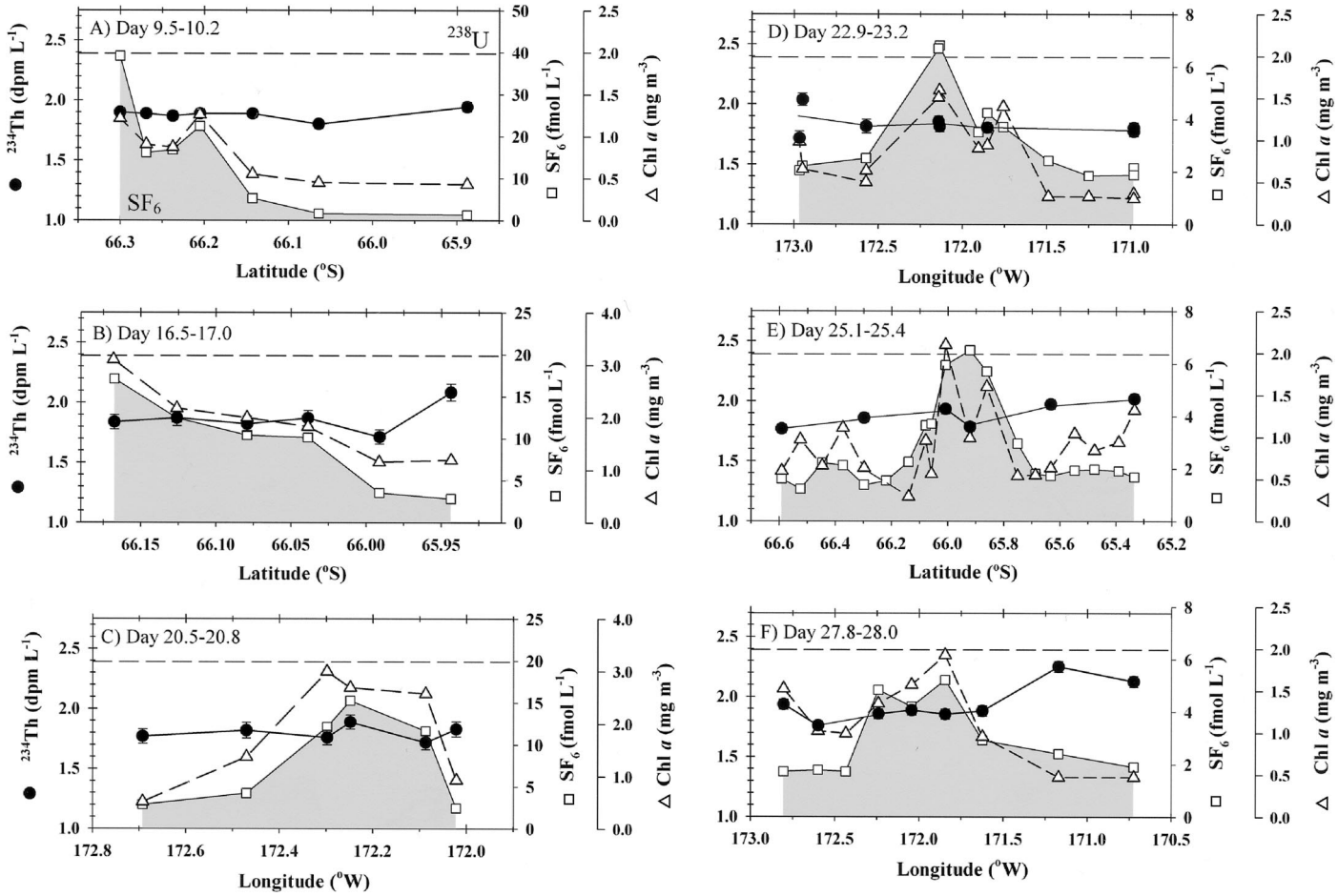

Fig. 1. A time series of six surface transects of total ^{234}Th activity, Chl *a* concentration, and SF_6 concentration (squares and shading) collected during SOFeX. The time over which sampling took place is noted in the upper left of each panel. Dashed horizontal line represents ^{238}U activity, and ^{234}Th $<$ ^{238}U indicates export on sinking particles. Samples were collected either from 25 m or the surface, and on one occasion, selected stations had ^{234}Th data from both depths for comparison (day 22.9–23.2). Note that the SF_6 vertical scale decreases with time because of natural dilution and air–sea losses of this tracer. Chl *a* scale also changes to show progression of biomass response relative to SF_6. Transects are plotted against either latitude or longitude depending on predominant orientation of the transect (*see Fig. 2 map*).

the patch center. Also, on the transect of day 28 (Fig. 1F), high Chl *a* was observed along the western edge (1.6 mg m^{-3}), decreasing outside the patch toward the easternmost stations, where some of the highest ^{234}Th activities were found.

The clear relationship between iron addition and Chl *a* in the surface transect data was not reflected in ^{234}Th, which displayed relatively invariant activities across the patch center along every individual transect (Fig. 1). However, a subtle decrease in average ^{234}Th activities in the patch relative to the ^{238}U activity is seen over time (to be discussed later in the context of the vertical profiles), and some small-scale variability in ^{234}Th along the transect is unrelated to the iron-fertilized patch.

The sampling of both high– and low–Chl *a* waters and more variable ^{234}Th activities outside the patch exemplifies the natural heterogeneity of the Southern Ocean during the austral summer. This heterogeneity also highlights the difficulty in defining an OUT control station among these local variations in biomass, ^{234}Th, and biogeochemistry. Although we lump all profiles from low-SF_6 waters as OUT stations, this variability should be kept in mind as we compare temporal changes in the OUT control stations with the Lagrangian time series sampling of the SF_6-tagged IN stations.

Time series profiles—At the start of SOFeX (t = 5.8 d), there was a sharp pycnocline at the base of the mixed layer (30–35 m), below which a broad temperature (T) minimum extended from the base of the mixed layer to 80 m (Fig. 3A). Density changes are driven primarily by salinity (S), which increased gradually below the mixed layer. These T/S properties are common to the Southern Ocean waters south of the Southern Antarctic Circumpolar Current Front along 170°W (Morrison et al. 2001) and were seen at all stations inside and outside the patch. The T/S structure is formed after the local retreat of the sea ice in the spring (starting around late November at this location), whereby warming of the lower salinity meltwaters creates a gradually shoaling and warmer mixed layer overlying the near freezing waters below. During SOFeX, the depth of the mixed layer in-

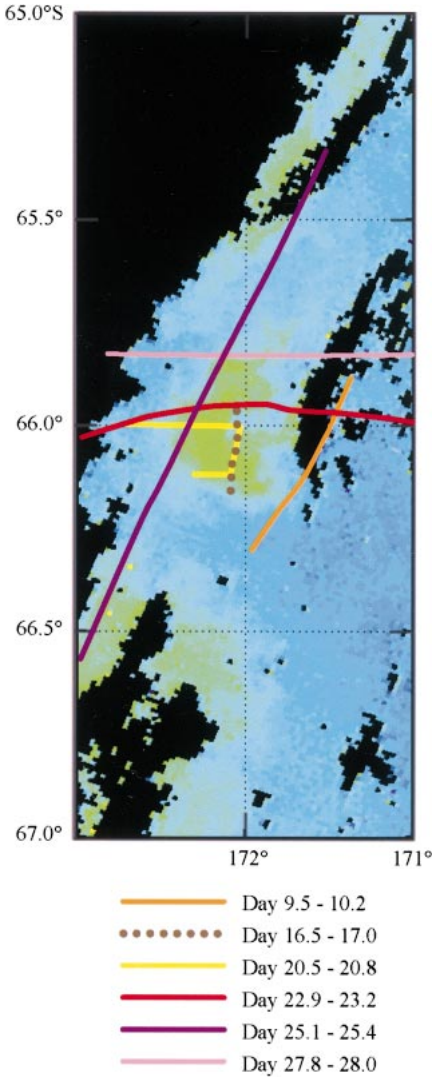

Fig. 2. Map of SOFeX site showing relative locations of six transects sampled in Fig. 1. These transects were collected over a 20-d period and represent different stages of the evolving and drifting patch (Fig. 1). For reference, the clearest satellite ocean color image for 16 February 2002 is overlain on these transects to show the relative scale of the patch, but note that both the location of the patch and its aerial extent would have changed throughout the experiment.

creased over time to ~50 m both IN and OUT of the patch because of a series of storms (Goldson 2004). These storms also reduced the vertical extent of the temperature minimum. The hydrographic changes recorded in the two final IN and OUT profiles from SOFeX (Fig. 3B,C) are characteristic of the changes observed in the complete data set (Bishop et al. 2004; Coale et al. 2004).

At the start of SOFeX, nutrient concentrations were high ($NO_3 > 25$ μmol L^{-1}; $Si(OH)_4 > 60$ μmol L^{-1}) and biomass was low (Chl $a < 0.5$ mg m^{-3}), which is typical of austral summer conditions for this HNLC region (Morrison et al. 2001). Previous SeaWiFS (Sea-viewing Wide Field-of-view Sensor) satellite estimates of surface chlorophyll along 170°W suggest that higher Chl *a* and primary productivity would have been found in December and early January in association with ice edge blooms prior to the initiation of SOFeX (Buesseler et al. 2003). During these early blooms, maximum Chl *a* concentrations on the order of 0.8–1.4 mg m^{-3} have been seen, which are roughly twice the values seen here at the start of SOFeX. The relatively low ^{234}Th activities observed in the OUT stations also suggest that the experiment began after particle export likely associated with the December/January ice edge blooms.

One of the major characteristics of SOFeX and previous Southern Ocean iron fertilization experiments has been a slow response to iron in terms of biomass accumulation, mainly because of the slower metabolism of phytoplankton in the cold Antarctic waters. Thus, although a physiological response to Fe, as indicated by an increase in photosynthetic efficiency, was observed after only a few days, increases in biomass were not detected until 5–7 d after Fe was first added (Boyd and Abraham 2001; Coale et al. 2004). During SOFeX, biomass increased to >2–3 mg m^{-3} Chl *a* within the patch after 15–20 d but remained <0.5 mg m^{-3} Chl *a* outside the patch throughout the experiment.

At the start of SOFeX ($t = 5.8$ d), the lowest ^{234}Th activities were observed within the mixed layer (Fig. 3A). This initial ^{234}Th : ^{238}U disequilibrium indicates a previous flux of particles associated with the natural bloom cycle. ^{234}Th activities increased with depth to values greater than ^{238}U (>2.4 dpm L^{-1}), indicative of remineralization. Thus at the start of SOFeX, the site had already experienced a vertical flux of particles carrying ^{234}Th out of the mixed layer, accompanied by remineralization of some of these particles at depths of 80–120 m.

Overall, upper ocean (0–50 m) ^{234}Th activities ranged between 1.7 and 2.1 dpm L^{-1} during the course of the experiment, and large changes over time were not obvious. To put these ^{234}Th data in context, we have seen decreases in ^{234}Th activities as large as 1 dpm L^{-1} associated with the end of the spring bloom in the North Atlantic (Buesseler et al. 1992) and the end of the SW Monsoon in the Arabian Sea (Buesseler et al. 1998). Thus, the lack of a stronger inverse correlation between surface SF_6 and ^{234}Th, is evidence that during the 4-week occupation of the SOFeX bloom, surface ocean export was not particularly elevated, or at least was small relative to other observations of particle export associated with natural blooms from other regions.

The IN station time series was characterized by a small decrease in mixed-layer ^{234}Th and a penetration of the growing deficit to greater depths over the course of the experiment (*see* time series integrals that follow). By the end of SOFeX, mixed-layer ^{234}Th activities had decreased slightly both IN and OUT (Fig. 3B,C). However, two important differences were observed between the IN and OUT station time series: (1) the vertical extent of the ^{234}Th disequilibrium was greater at IN stations and (2) the excess ^{234}Th feature at 80–120 m present at the beginning of the experiment persisted at OUT stations, but eventually disappeared at IN stations.

To rule out physical mixing processes as a potential explanation for these changes, we plotted the final IN and OUT ^{234}Th activities against density (Fig. 4). Within the lowest density surface waters, there was little difference in ^{234}Th

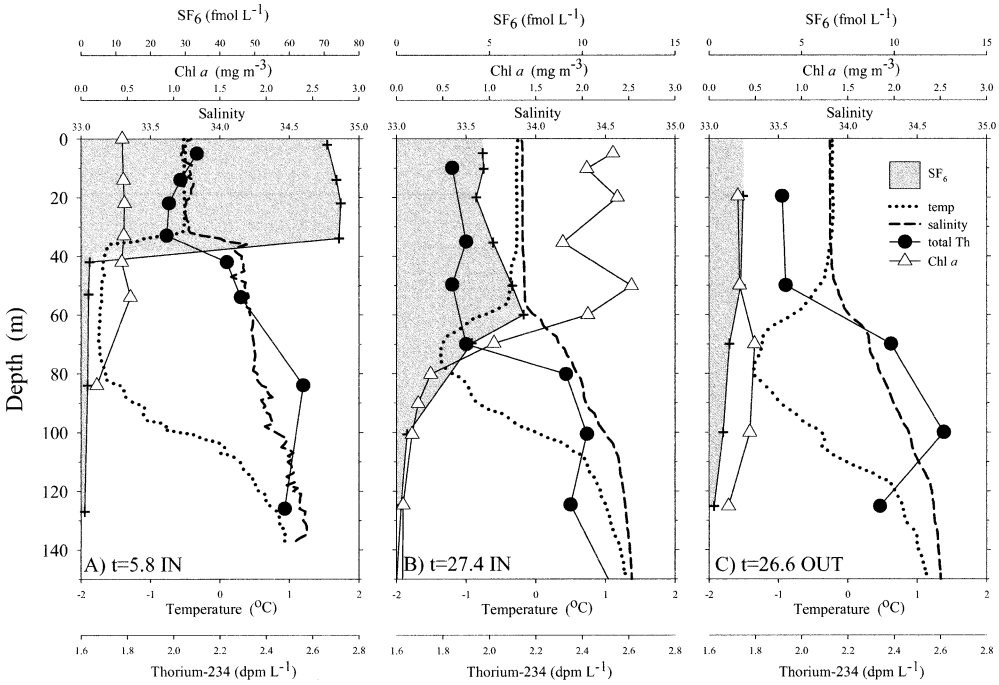

Fig. 3. Depth profiles from (A) the first IN station (t = 5.8 d), (B) the last IN station (t = 27.4 d), and (C) the last OUT station (t = 26.6 d). Plotted against depth are conductivity–temperature–depth (CTD) data for temperature and salinity. Total ^{234}Th activity and Chl *a* concentration data are from same CTD cast. The last IN and last OUT SF_6 samples (squares and shading) are also from these same casts, whereas SF_6 from t = 5.8 d are from a co-located station. All horizontal scales are constant, except for SF_6, which is decreased for the last two stations because of lower SF_6 late in the experiment. Details of ship and station identification can be found in Web Appendix 1.

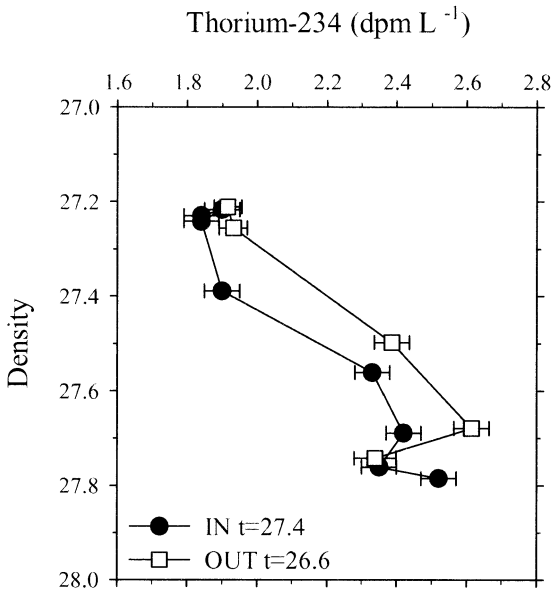

Fig. 4. Total ^{234}Th activities plotted against density for the last IN station and last OUT station. ^{234}Th activities are plotted with associated error.

activity, consistent with the lack of IN compared with OUT differences observed in context of the surface transect data. By the end of SOFeX, we observed 0.1–0.2 dpm L^{-1} lower total ^{234}Th activities (mean error = 0.05 dpm L^{-1}) within the patch, extending to densities of 27.7, which includes depths below the mixed layer down to the peak in ^{234}Th excess at 80–120 m. These changes cannot be explained by subtle differences in the IN compared with OUT hydrography and must therefore be a result of the SOFeX Fe release. We conclude that this small decrease in total ^{234}Th activity over time is direct evidence of enhanced particle flux within the SOFeX patch.

As noted above, an unusual feature of the early IN stations and all OUT stations was the presence of excess ^{234}Th at depths of 80–120 m (Fig. 3A,C). Because the only in situ source of ^{234}Th in seawater is ^{238}U decay, total ^{234}Th activities can never exceed those of ^{238}U unless some additional nonlocal source exists, in this case, from sinking particles either releasing ^{234}Th to the dissolved phase or disaggregating into suspended material. Interestingly, excess ^{234}Th remained unchanged in the OUT stations, yet for the IN stations, the excess ^{234}Th generally disappeared by the end of the experiment (Fig. 5). This indicates that some process below the mixed layer responded to the development of the bloom by allowing a greater fraction of the ^{234}Th on sinking particles to reach greater depths. This implies either a change in the nature of the sinking particles (i.e., faster settling, less labile), a subsurface change in the processes responsible for

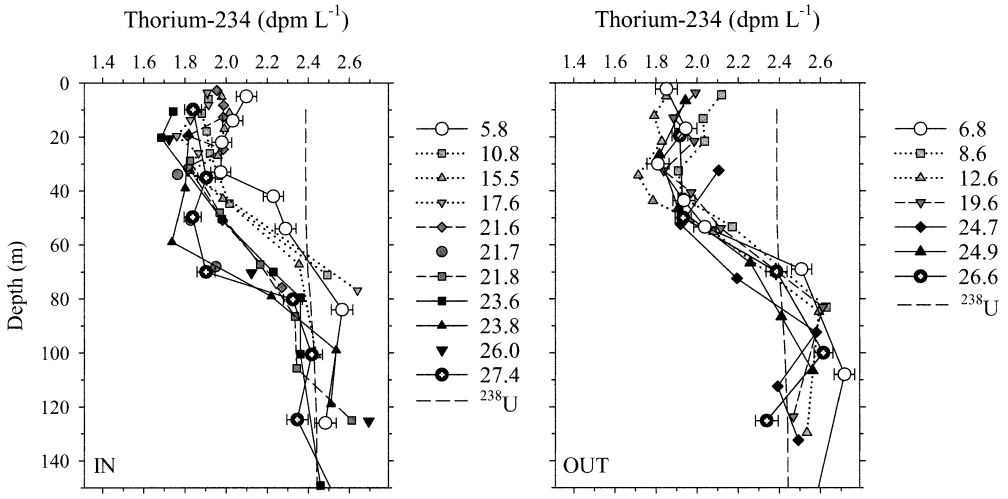

Fig. 5. Complete SOFeX total ^{234}Th time series for IN and OUT data. Vertical dashed line is ^{238}U calculated from measured salinity.

remineralization (e.g., a migration of zooplankton that consumes sinking particles to shallower depths as the bloom develops within the mixed layer), or both.

The reproducibility of the excess thorium feature in the OUT stations and the temporal changes IN provide unique insights into the extent of remineralization below both the natural and iron-induced biological communities. The excess ^{234}Th does not tell us the exact process responsible for the decrease in particle flux—be it physicochemical, microbial, or zooplankton driven—but further examination of this feature in context of the broader SOFeX data sets will be warranted once these results are available. However, it should be noted that the SOFeX sampling program was focused primarily on the expected surface water response to iron and not on this subsurface change in the particle cycle; thus, no specific experiments designed to follow this deeper feature were conducted.

From this detailed time series data set, we can quantify temporal changes in particle flux derived from ^{234}Th : ^{238}U disequilibrium. All of the SOFeX total ^{234}Th profiles from the South Patch have been plotted (Fig. 5A,B and the data provided in Web Appendix 1 at http://www.aslo.org/lo/toc/vol_50/issue_1/0311a1.pdf). This single data set comprises the most extensive suite of ^{234}Th data ever collected at a single site within a relatively short 4-week time period. Because the IN data were collected as part of the SOFeX Lagrangian sampling of the fertilized patch, they also provide us with a true time series record of the development of the SOFeX bloom.

Time series integrals—The flux of ^{234}Th on sinking particles can be determined by solving for the balance of ^{234}Th sources and sinks with the mathematical expression in Eq. 1,

$$\partial^{234}\mathrm{Th}/\partial t = (^{238}\mathrm{U} - {}^{234}\mathrm{Th})\cdot\lambda - P + V \qquad (1)$$

where ∂Th/∂t is the change in ^{234}Th activity with time, ^{238}U is the uranium activity determined from its conservative relationship with salinity (^{238}U [dpm L^{-1}] = 0.071·S; Chen et al. 1986), ^{234}Th is the activity of total ^{234}Th, λ is the decay constant for ^{234}Th (=0.0288 d^{-1}), P is the net export flux of ^{234}Th on sinking particles, and V is the sum of advective and diffusive ^{234}Th fluxes.

From the integral, or depth-averaged ^{234}Th and ^{238}U activities, P (in terms of dpm m^{-2} d^{-1}) can be solved for any given depth horizon. Typically with single profiles of ^{234}Th at a given site, steady state is assumed (∂Th/∂t = 0). As can be seen mathematically in Eq. 1, a negative ∂Th/∂t requires a larger ^{234}Th flux in order balance the production and decay rates. The changes in ^{234}Th activity (∂Th/∂t) following oceanic blooms can be one of the largest terms in Eq. 1 and should always be considered in these settings (Tsunogai et al. 1986; Buesseler et al. 1992; Wei and Murray 1992; Cochran et al. 1997). Thus, a time series sampling approach is essential when applying ^{234}Th in open ocean iron enrichment studies, given the expectation of a particle flux response to the iron addition (Bidigare et al. 1999; Charette and Buesseler 2000).

In order to calculate fluxes over time at different depths from a nonuniform vertical sampling grid, the average total ^{234}Th activities (dpm L^{-1}) were binned into five depth integrals (0–25, 0–50, 0–75, 0–100, and 0–125 m) because, to calculate the flux at 25 m, one needs to know the average ^{234}Th activity from the surface to 25 m, for 50 m from the surface to 50 m, and so on. As detailed in Buesseler et al. (1992, appendix A), to estimate ∂Th/∂t for a non–steady state (NSS) solution to Eq. 1, one can use the linear change in ^{234}Th activity over the course of time series measurements to estimate ∂Th/∂t. For the IN data, we measured a statistically significant linear decrease in average total ^{234}Th activities against time during SOFeX for all depth integrals (Fig. 6). As expected from the profiles, the average ^{234}Th activity increased with the deeper depth integrals. Also, the time series decreases were greatest for the intervals of 0–75 and 0–100 m IN, which include the interval where the ^{234}Th remineralization peak progressively disappeared (Table 1). Although this slope has some variability, especially in the upper 25–50 m, the decrease over 28 d is statistically greater than the measurement error, and most data fall within the

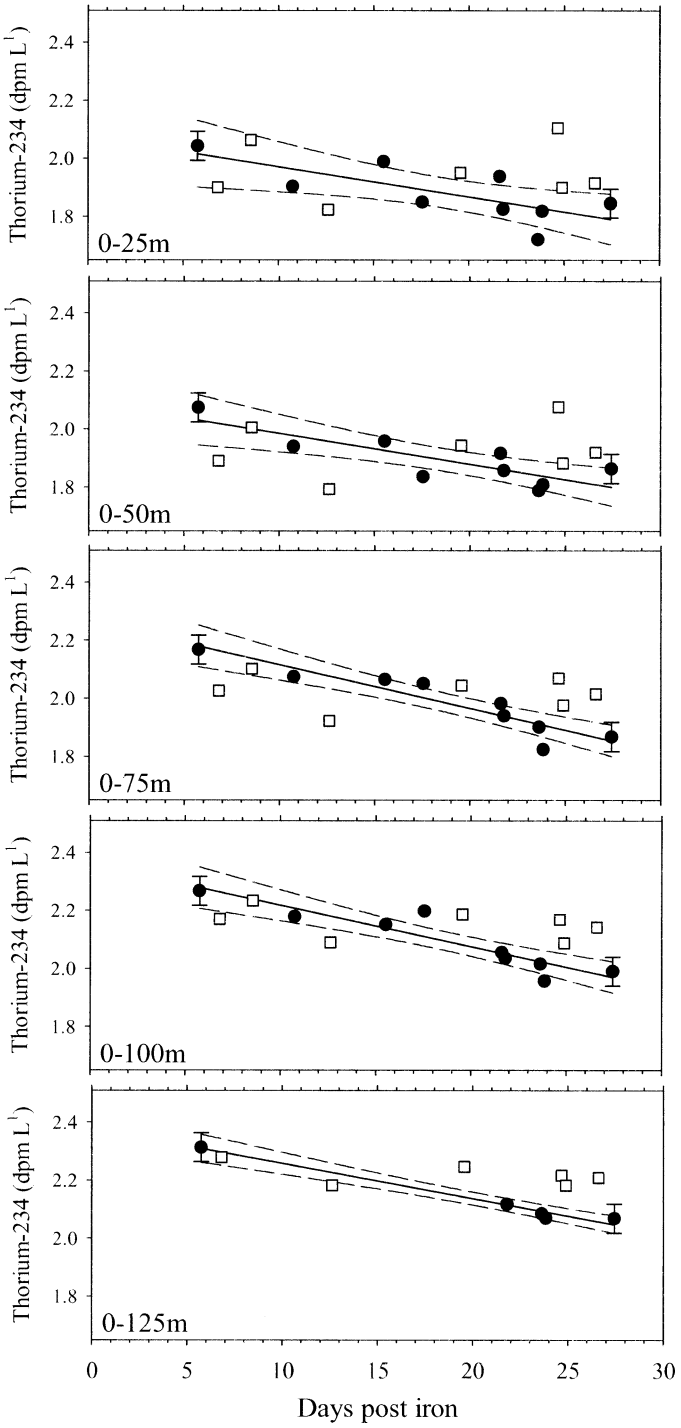

Fig. 6. Time series of the integrated total ^{234}Th activity from progressively deeper layers for SOFeX. All data with more than three vertical sampling points were plotted, and depth was averaged by trapezoid integration (data in Web Appendix 1). Solid line is the best fit to a linear decrease in total ^{234}Th versus time IN, and dashed lines represent 95% confidence limits around this slope (r^2, slopes, and errors provided in Table 1). Errors on the ^{234}Th activity measurement are shown for the first and last IN point for each depth interval.

Table 1. Time series total ^{234}Th.

Depth range (m)	Slope ∂Th/∂t	% error	r^2
0–25	−0.010	35	0.54
0–50	−0.011	25	0.69
0–75	−0.015	15	0.86
0–100	−0.014	16	0.85
0–125	−0.012	9	0.98

95% confidence limits of the linear fit. The calculated standard error on the slope of these curves ranges from <10% for the 0–125-m depth integral to 35% for the 0–25-m layer (Table 1).

The results in Table 1 allow us to quantify ∂Th/∂t in Eq. 1 and the error associated with this fit, so that we can apply a NSS solution to Eq. 1 for the IN stations. The OUT data are also plotted (Fig. 6), but no linear fit is drawn because none of these data had slopes statistically different from zero ($r^2 < 0.15$). This lack of change in ∂Th/∂t OUT is one of the biggest uncertainties in the interpretation of the OUT flux data because, as seen in these transects, there is natural variability in ^{234}Th outside of the patch, and a true Lagrangian control was not sampled.

^{234}Th fluxes—Using the time series integrals of total ^{234}Th activity and Eq. 1, we can calculate the evolving ^{234}Th flux patterns with depth and time at both IN and OUT stations. For both IN and OUT stations, we assume steady state conditions at the start of SOFeX (i.e., ∂Th/$\partial t = 0$) and use the measured ^{234}Th activity for any given depth integral to calculate the flux. For the IN stations, we applied a NSS solution to Eq. 1 beginning with day 10 (we assume there was no significant decrease in ^{234}Th until this second sampling point). We use the linear fit to the ^{234}Th activity decrease with time as our estimate of ∂Th/∂t during the entire experiment (Table 1) and to calculate the average ^{234}Th activity for any depth integral on a given day. For OUT stations, ^{234}Th showed no clear decrease with time; hence, we calculated the ^{234}Th flux with the use of a steady state model throughout the experiment. Errors on the fluxes are derived from propagating errors from the slope ∂Th/∂t and the error on the average ^{234}Th activity.

Using these assumptions, we plot the flux profiles at the start (day 6 IN and day 7 OUT), day 10, day 20, and end (day 27) in Fig. 7A,B. At the start of SOFeX, IN and OUT fluxes were similar, ranging from 250 to 300 dpm m^{-2} d^{-1} at 25 m, increasing to a maximum of 500–700 dpm m^{-2} d^{-1} at 75 m, and decreasing to values of 300–400 dpm m^{-2} d^{-1} at depths of 100–125 m (Fig. 7A,B). The largest increase in ^{234}Th flux with depth is found between 25 and 75 m for the IN stations (Fig. 7A). Compared with the start of the experiment (at both IN and OUT stations), ^{234}Th fluxes at the end between 75 and 125 m increased nearly fivefold to 2,300–2,800 dpm m^{-2} d^{-1}. At the OUT stations, the ^{234}Th flux distribution with depth was similar over time, and the magnitude of the ^{234}Th flux remained low (Fig. 7B).

The most significant finding of this study was the observed ^{234}Th flux increase IN, which is strong evidence of

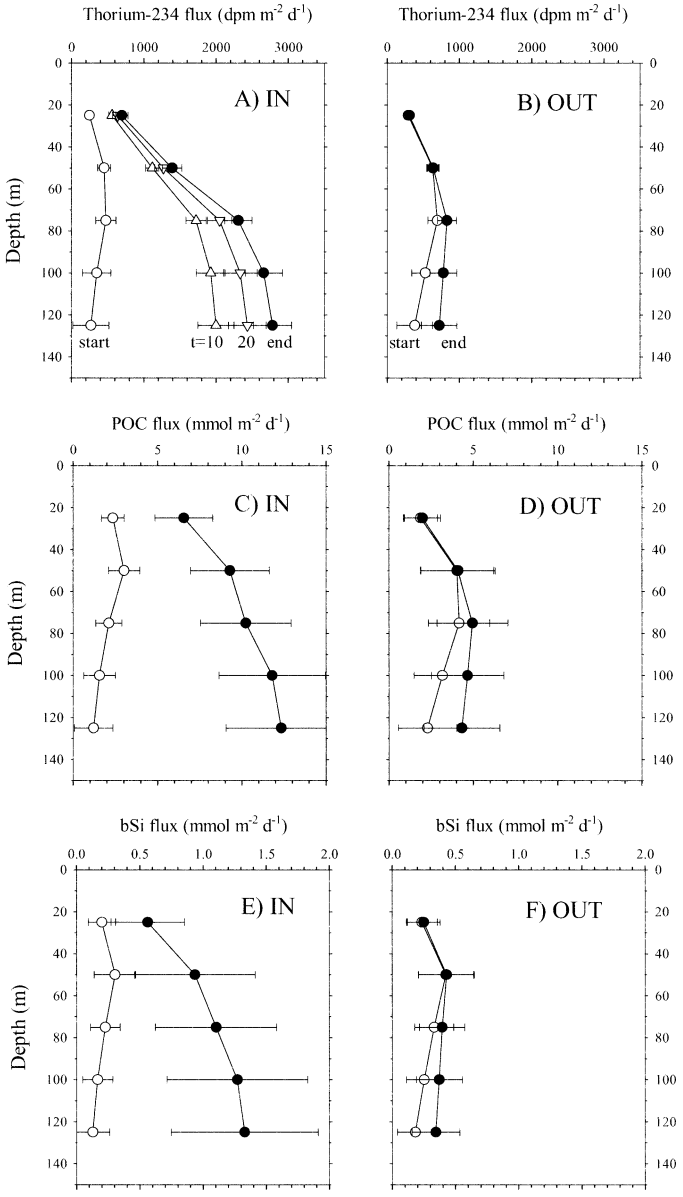

Fig. 7. Plots of particle flux versus depth for (A) ^{234}Th IN and (B) ^{234}Th OUT (dpm m^{-2} d^{-1}), (C) POC IN and (D) POC OUT (mmol m^{-2} d^{-1}), and (E) $bSiO_2$ IN and (F) $bSiO_2$ OUT (mmol m^{-2} d^{-1}). Plotted are the estimates for each 25-m layer at the start of the experiment (day 5–6, open circle) and end (day 27, filled circle) of SOFeX; errors on this flux estimate are shown by the horizontal error bars. For ^{234}Th IN, estimates of the flux on days 10 and 20 are also plotted. Complete flux data can be found in Table 2.

enhanced particle export in response to an open-ocean iron fertilization experiment (Buesseler et al. 2004). In addition, an unexpected change in the ^{234}Th flux occurred below the iron-enriched waters. Although the ^{234}Th remineralization peak at 80–120 m persisted at the OUT stations for the entire experiment, this feature essentially disappeared at the IN stations by day 15.

These findings have several important implications. Not only did iron fertilization enhance particle flux within the upper fertilized layers, but it also might have influenced the fate of these materials once they left the surface waters. In the latter case, elements that left the upper 50 m in association with sinking particles might be more efficiently transported to depth after fertilization. Possible explanations for this effect include changes in heterotrophic processes responsible for particle break-up and consumption, changes in the nature of the material leaving the euphotic zone that might lead to more efficient transport to depth (i.e. more rapidly sinking or less labile particles), or a combination of mechanisms.

Effect of physical transport on ^{234}Th flux assessment—The influence of vertical mixing on the ^{234}Th flux model can be substantial, particularly in high upwelling sites and times, such as the coastal Arabian Sea at the onset of the monsoon (Buesseler et al. 1998) or in equatorial regions where upwelling can increase the calculated ^{234}Th fluxes by up to a factor of two (Buesseler et al. 1995; Dunne and Murray, 1999). Horizontal transport of ^{234}Th also has been shown to be particularly important in coastal regions (Gustafsson et al. 1998; Benitez-Nelson et al. 2000; Charette et al. 2001). With the exception of loss across the air–sea interface, SF_6 behaves conservatively in seawater. As such, the temporal evolution of the SF_6 tracer along and across isopycnals can be used to determine the horizontal and vertical exchange rates, respectively, which are applied to ^{234}Th.

During SOFeX, the temporal spread of SF_6 across the lower boundary of the mixed layer was used to derive a rate of vertical diffusivity of approximately 0.3 cm^2 s^{-1}. Details of this study are presented in Goldson (2004). Because the activity of ^{234}Th increases with depth, its supply via vertical processes would provide an additional source to shallower layers; thus, by ignoring this process, we would underestimate vertical fluxes. Given this rate of vertical diffusion and the vertical gradient of ^{234}Th below the surface disequilibrium, we estimated that vertical mixing processes could supply ~100 dpm m^{-2} d^{-1}. At 100 m inside the patch at the end of SOFeX, this vertical source of ^{234}Th to the mixed layer was <5% of the total ^{234}Th flux and fell within the overall error of the model.

Patch dilution can help us estimate the effect of horizontal mixing on the ^{234}Th activity balance. Dilution has been calculated for SOFeX both by physical strain methods (Abraham et al. 2000) and by looking at the losses of SF_6 over time, corrected for outgassing (Coale et al. 2004). Both methods agree fairly well, and here we use an average dilution rate of 0.05 d^{-1} derived from SF_6 (range 0.03–0.07 d^{-1}). Dilution can affect geochemical budgets differently, depending on the time series response and IN–OUT gradients and, in the case of ^{234}Th, the relative magnitude of the physical transport terms compared with the production and decay rates of ^{234}Th (Eq. 1). Using the 0–50-m integrated total ^{234}Th data (Fig. 6) to calculate weekly IN–OUT gradients, we estimated that dilution would affect our 50-m fluxes by −140, +50, and +240 dpm m^{-2} d^{-1} during weeks 2, 3, and 4, respectively. The magnitude of this adjustment is small relative to the NSS fluxes, and because we do not have adequate four-dimensional coverage to assess horizontal gradients very reliably, we chose not to adjust our NSS fluxes by these small corrections. Note also that total errors on the

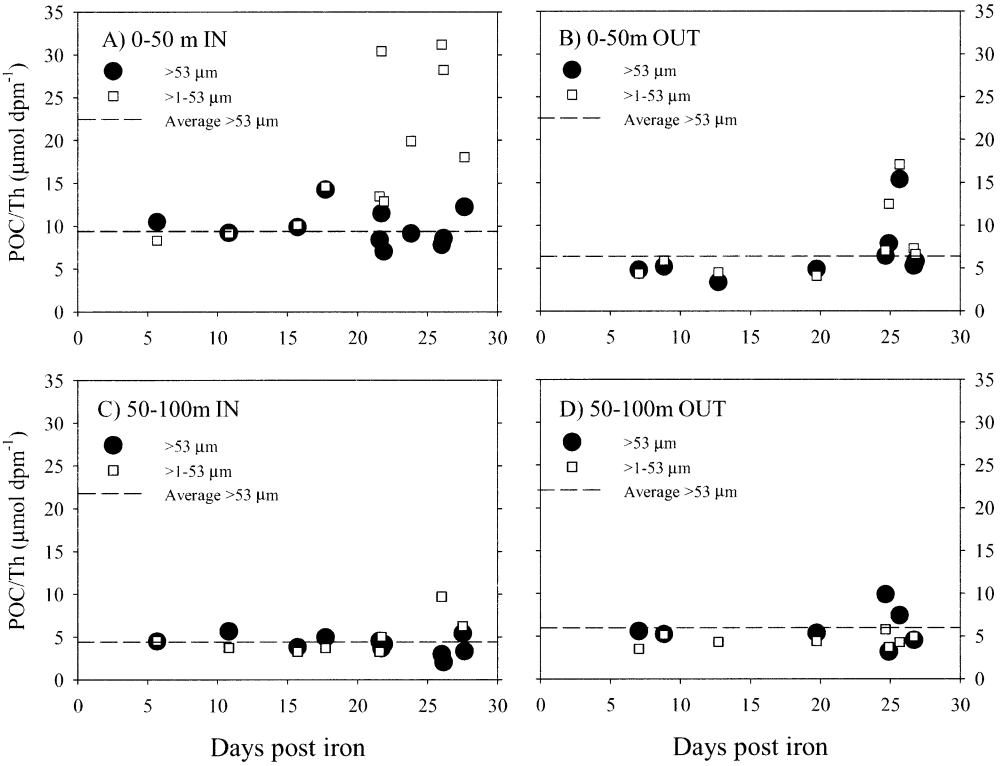

Fig. 8. Time series progression of POC : ^{234}Th on large (>54 μm) and small particles (1–54 μm). These are separated by depth—(A, B) 0–50 m, (C, D) 50–100 m—and by station—(A, C) IN, (B, D) OUT. The average value for the >54-μm particles for the entire time sequence is shown by a horizontal dashed line.

elemental fluxes are ±25–50%, so we don't consider these dilution effects on the ^{234}Th flux to be significant within these errors.

Flux of particulate organic carbon—If the flux of ^{234}Th on sinking particles is known, then the export flux of POC and other constituents can be estimated from knowledge of the ratio of a given constituent, *E*, to ^{234}Th in particles by Eq. 2.

$$\text{flux } E = E/^{234}\text{Th} \cdot \text{flux } ^{234}\text{Th} \quad (2)$$

This empirical approach assumes that we know the flux of ^{234}Th accurately and that the particulate *E* : Th ratio is representative of sinking particles at the same time and depth of interest. During SOFeX, the elemental ratios of POC, PON, and $bSiO_2$ compared with ^{234}Th on sinking particles were derived from size-fractionated samples collected with the use of in situ pumps (Web Appendix 2 at http://www.aslo.org/lo/toc/vol_50/issue_1/0311a2.pdf). For POC : Th, we now have considerable background on its variability (Buesseler 1998) and generally find decreasing ratios with depth. Higher ratios are commonly found during blooms and at high latitudes, where large diatoms and *Phaeocystis* blooms are common. Although the exact processes that control this ratio are not known, these two basic features can be explained by preferential recycling of POC from particles as they sink. This leads to lower POC : Th and higher POC : Th being associated with larger cells that have lower surface area to volume ratios because ^{234}Th is a surface-reactive element and POC varies as a function of cell volume. We assume that the larger particle size classes have higher settling velocities and use this ratio in our elemental flux calculations, but we also examine the finer suspended material to put some bounds on possible errors associated with this assumption.

During SOFeX, time series particulate samples were commonly collected in pairs: one sample from within the mixed layer and one from below. At some of the later stations, we also had three or four points of depth resolution. POC : Th ratios averaged just under 10 μmol dpm^{-1} in the upper 50 m on the larger (>54 μm) size class, with little change during the course of SOFeX (Fig. 8A). For the small particles (>1 to 54 μm), we observed ratios similar to the large particles for the first 2–3 weeks of SOFeX, but strikingly higher ratios (>30 μmol dpm^{-1}) during the fourth week of the experiment. At depth, the same ratios were much lower (4.4 μmol dpm^{-1}) and similar between the two size classes throughout these observations (Fig. 8C). The OUT data displayed more similar POC : Th ratios between the two particle size classes and with depth (Fig. 8B,D). There was evidence of slightly higher POC : Th late in the upper 50 m OUT, but not as large as the changes IN.

We attribute the temporal increase in POC : Th ratios IN to changes in the iron-induced phytoplankton bloom because the community response was greatest for the larger (>20 μm) diatoms after the addition of iron (Coale et al. 2004).

If the material caught on the 1-μm filter represents fresh biogenic material between 1 and 54 μm, then it implies that over time, the increase in POC : Th attributable to these new diatom cells had not yet affected the larger aggregates in the >54-μm fraction. Also, there was no evidence of the POC : Th ratio increase at depth over time, suggesting that the diatoms had not yet aggregated or sunk to depth. This result is consistent with the observation that the SOFeX bloom had not reached a stage of high export characteristic of bloom termination and agrees with the general findings that Chl *a* and POC concentrations had leveled off by weeks 3–4. There was a lack of any measurable Fe stress (as evidenced by continued high photosynthetic efficiency) even at the end of our 28-d observation period (Coale et al. 2004).

As early as day 6, when there was not yet any evidence of a decline in total ^{234}Th activity within the patch, particulate ^{234}Th activities of >1–54 μm had decreased slightly in the upper 50 m (0.35 dpm L^{-1} IN compared with 0.53 dpm L^{-1} OUT on 1–54-μm particles; Web Appendix 2). During a previous Southern Ocean iron fertilization experiment, we observed a similar decrease in the partitioning of ^{234}Th onto smaller particles (Charette and Buesseler 2000) and can only speculate as to the cause. One response to added Fe might be an increase in production of organic ligands by the biota that complex Fe and other trace metals (Bowie et al. 2001). It is possible that these ligands were competing for adsorbed thorium atoms, which would explain the decrease of ^{234}Th in the particulate pool (Santschi et al. 2003). This IN patch decrease in particulate ^{234}Th activities coincided with a smaller IN patch increase in POC concentration (2.5–3.0 μmol L^{-1} by day 6); therefore, the higher shallow POC : Th ratios at IN stations were driven by both of these concentration changes. A change in ^{234}Th partitioning does not affect the ^{234}Th flux directly, and the total activities IN and OUT were similar during the first 1–2 weeks of the experiment.

We assume from theory that the larger particles are the best representation of the sinking particle pool and thus use the >54-μm data to calculate our elemental fluxes. However, the similarity in the POC : Th ratio between the >1–54-μm and >54-μm particles at depth during the entire experiment and in surface waters at the beginning of SOFeX provides rather narrow constraints on the possible range of the POC : Th ratio for any particular time and depth; hence, the magnitude of the POC flux is tightly constrained by these data.

Filtration is an operational procedure that can introduce collection biases from sampling and experimental conditions and particle type. Methods-related differences have been found, for example, in the concentration of POC measured by bottle and in situ pump methods (Moran et al. 1999; Gardner et al. 2003). We contend that because we measure both POC and ^{234}Th together on the same filter matrix, collected with a single method, the only possible methods bias would be if we had missed a class of sinking particles with a different POC : Th ratio ***and*** these missing particles dominated the local particle flux. Alternatively, if the filtration caused the loss of dissolved organic carbon (DOC) from cells, that loss would have to be large and the material would have to have a dramatically different POC : Th ratio in order to significantly bias the flux estimate. It is important to note that the total range in observed POC : Th ratios should not be used as an estimate of the accuracy of the method (Moran et al. 2003). With this empirical approach, it is only appropriate to apply the POC : Th ratio characteristic of the particles at the base of any given depth integral to calculate the POC flux at that depth (Benitez-Nelson and Charette 2004). The range in observed POC : Th ratios at a given depth and time are considerably smaller than the total range of all time series POC : Th data for all depths (Fig. 8).

We calculated the flux of POC for IN and OUT stations by fitting the profile of >54-μm POC : Th ratios, assuming a linear decrease between the mixed layer and 75 m, and using the average of the 50–100-m POC : Th data below that point (Fig. 9; Table 2). Because the IN patch POC flux is essentially the product of Figs. 7A and 9A, the flux profile for POC increases substantially both below the Fe patch at 50 m and in response to the higher ^{234}Th fluxes below that more than compensate for the decrease in POC : Th in this depth zone (Fig. 7C). POC fluxes at the base of the mixed layer (50 m) of the patch increased from 3 $\pm$ 0.9 mmol m^{-2} d^{-1} at the start to 9.3 $\pm$ 2.3 mmol m^{-2} d^{-1} by our last observation. Flux increases were largest below this layer, increasing from 1.6 $\pm$ 0.9 to 11.8 $\pm$ 3.2 mmol m^{-2} d^{-1} at 100 m from the start to the end of the experiment (Fig. 7C; Table 2). At the OUT stations, POC fluxes increased from about 2 to 5 mmol m^{-2} d^{-1} in the mixed layer and decreased below that layer but did not vary much with time (Fig. 7D). The errors estimated here for the POC flux (1–3 mmol m^{-2} d^{-1}) were propagated from both the error on the ^{234}Th flux model (which increases with depth) and variability in POC : Th data. For the POC : Th error, we used the standard deviation from the >54-μm POC : Th samples collected at the depth of interest (averaging all time points because we did not see any statistically significant temporal trend for the >54-μm particles); in general, this variability decreased with increasing depth (Table 2).

We do not report here the flux of PON specifically because, by using the ratio of C : N reported in Web Appendix 2, one can simply convert from C to N units. This ratio (moles) on the >54-μm particles averages 6.0 in the upper 50 m and 6.9 between 50 and 100 m at the IN stations, and is similar OUT.

Biogenic silica flux—The flux of biogenic silica in the upper 125 m was estimated in a manner exactly analogous to that described for POC. The $bSiO_2$: Th ratio for the >54-μm particles in each depth horizon showed no significant change with time but varied by almost a factor of two between the surface and 100 m (Web Appendix 2). Thus, we applied a depth-varying, but temporally constant $bSiO_2$: Th ratio to calculate $bSiO_2$ flux from thorium flux for each 25-m depth integral from the surface to 125 m (Table 2; Fig. 9). The $bSiO_2$: Th ratio for each depth integral was calculated with the same interpolation scheme as described for POC : Th.

The flux of $bSiO_2$ at the base of the mixed layer (50 m) of the patch increased threefold during the experiment, rising from 0.2 $\pm$ 0.1 mmol Si m^{-2} d^{-1} at the start to 0.6 $\pm$ 0.3 mmol Si m^{-2} d^{-1} by our last observation. As with POC flux, the increase in the flux of $bSiO_2$ was greatest below the mixed layer at 100 m, where $bSiO_2$ export increased 6.5-fold

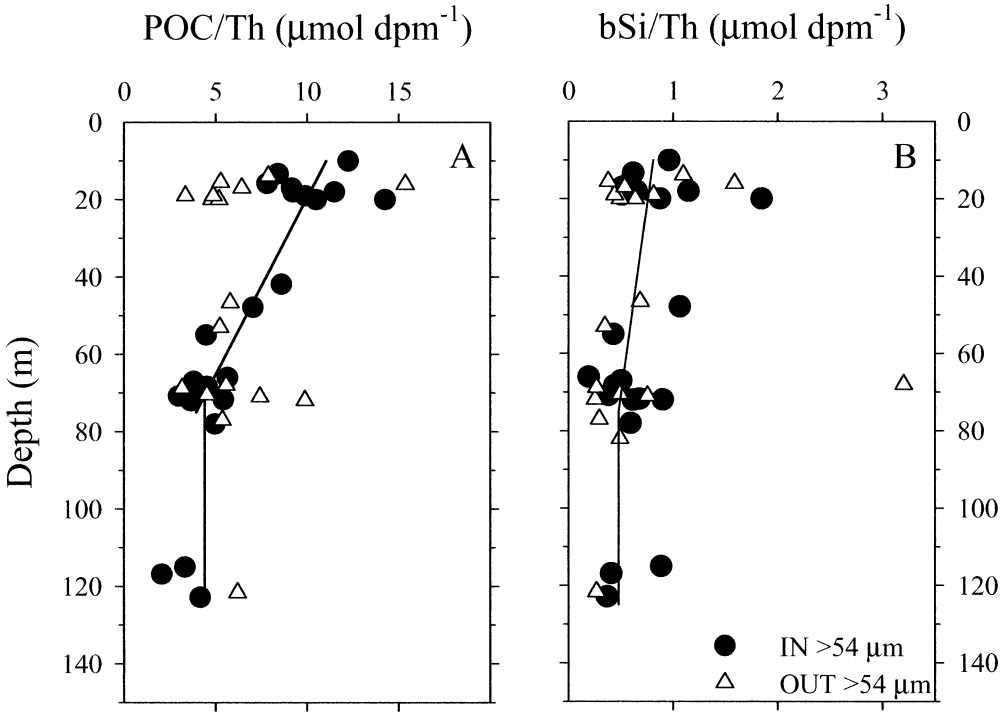

Fig. 9. Particulate ratios of (A) POC : ^{234}Th and (B) $bSiO_2$: ^{234}Th (both μmol dpm^{-1}) versus depth for large (>54 μm) particles. IN stations are shown by open circles. The solid line depicts the best fit used to calculate fluxes. OUT station data are shown only for comparison.

Table 2. Particle flux results.

	IN					OUT		
Depth (m)	Start*	Day 10	Day 20	End†	Ratio with Th (μmol dpm^{-1})	Start*	End†	Ratios with Th (μmol dpm^{-1})
^{234}Th flux (dpm m^{-2} d^{-1})								
25	249±44	563±49	638±68	697±84		291±41	309±41	
50	453±90	1117±90	1270±119	1392±137		630±82	639±82	
75	477±141	1725±140	2049±171	2309±189		694±131	826±131	
100	350±196	1926±198	2335±234	2662±259		528±188	778±188	
125	271±250	1999±249	2435±261	2783±263		382±246	721±246	
POC flux (mmol m^{-2} d^{-1})								
25	2.3±0.7	5.3±1.3	6.0±1.5	6.6±1.7	9.4±2.2	1.9±1.0	2.0±1.1	6.4±3.4
50	3.0±0.9	7.5±1.8	8.5±2.1	9.3±2.3	6.7±1.5	4.0±2.2	4.1±2.2	6.4±3.4
75	2.1±0.8	7.6±1.8	9.1±2.2	10.2±2.7	4.4±1.0	4.2±1.8	5.0±2.1	6.0±2.4
100	1.6±0.9	8.5±2.1	10.3±2.5	11.8±3.2	4.4±1.0	3.2±1.7	4.7±2.2	6.0±2.4
125	1.2±1.1	8.9±2.3	10.8±2.7	12.3±3.3	4.4±1.0	2.3±1.7	4.3±2.3	6.0±2.4
bSiO flux (mmol m^{-2} d^{-1})								
25	0.2±0.1	0.5±0.2	0.5±0.3	0.6±0.3	0.81±0.40	0.2±0.1	0.2±0.1	0.81±0.40
50	0.3±0.2	0.8±0.4	0.9±0.4	0.9±0.5	0.67±0.34	0.4±0.2	0.4±0.2	0.67±0.34
75	0.2±0.1	0.8±0.4	1.0±0.4	1.1±0.5	0.48±0.20	0.3±0.2	0.4±0.2	0.48±0.20
100	0.2±0.1	0.9±0.4	1.1±0.5	1.3±0.6	0.48±0.20	0.3±0.1	0.4±0.2	0.48±0.20
125	0.1±0.1	1.0±0.4	1.2±0.5	1.3±0.6	0.48±0.20	0.2±0.1	0.3±0.2	0.48±0.20

All times in days post-iron addition.
* Day 5.8 IN; day 6.8 OUT.
† Day 27.4 IN; day 26.6 OUT.

Table 3. Comparison between SOFeX and AESOPS: mixed layer properties and 100-m export fluxes.

	Units	SOFeX start, IN*	AESOPS KIWI 8 sta. 3	SOFeX end, OUT*	AESOPS KIWI 9 sta. 9	SOFeX end, IN*
Date		30 Jan 02	16 Jan 98	19 Feb 02	28 Feb 98	20 Feb 02
Latitude	°S	66.34	67.78	65.91	66.10	65.85
Longitude	°W	171.96	170.11	170.79	168.67	171.95
Temperature	°C	−0.55	0.44	−0.26	0.99	−0.29
Salinity		33.79	33.56	33.88	33.84	33.91
Mixed-layer depth	m	35.0	19.8	55.0	57.4	55.0
N, inorganic (NO_3, NO_2, and NH_4)	μmol L^{-1}	26.8	25.5	30.2	23.7	26.4
Silicate (dissolved)	μmol L^{-1}	64.8	60.1	55.5	52.8	50.4
Chl *a*	mg m^{-3}	0.63†	0.90‡	0.34§	0.18‖	3.8¶
Biogenic Si (particulate)	μmol L^{-1}	1.4	3.8	0.6	8.2	1.0
POC	μmol L^{-1}	7.8	16.1	15.2	13.8	nd
Primary production	mmol m^{-2} d^{-1}	43†	80‡	19§	17‖	82¶
Total ^{274}Th	dpm L^{-1}	2.02	1.14	1.92	0.85	1.86
POC : ^{234}Th at 100 m	μmol dpm^{-1}	4.4	5.2	6.0	5.2	4.4
^{234}Th flux at 100 m	dpm m^{-2} d^{-1}	350	3,066#	778	4,030**	2,662
POC flux at 100 m	mmol m^{-2} d^{-1}	1.6	16.0	4.7	20.8	11.8
bSi flux at 100 m	mmol m^{-2} d^{-1}	0.2	nd	0.4	6.9	1.3

* Start and end SOFeX dates correspond to first and last ^{234}Th sampling dates for all parameters, unless otherwise noted.
† 29 Jan 02, SOFeX M04, CTD13 integrated to 50 m.
‡ AESOPS primary productivity and Chl *a* estimated from SeaWIFS Chl *a* model (Buesseler et al. 2003).
§ 12 Feb 02 SOFeX M36, TM46 integrated to 50 m.
‖ Table 1 of Hiscock et al. (2003), mean of three subpolar regime stations.
¶ 14 Feb 02 SOFeX M43, TM52 integrated to 50 m.
# Steady state model station 3, 17 Jan 98 (Buesseler et al. 2001b).
** Non–stedy state model, 65.5–68°S, 20 Jan–01 Mar 98 average (Buesseler et al. 2001*b*).

from 0.2 ± 0.1 mmol Si m^{-2} d^{-1} at the start to 1.3 ± 0.6 mmol Si m^{-2} d^{-1} at the end of the experiment (Fig. 7E; Table 2). In contrast, the flux of $bSiO_2$ did not change in the upper 50 m at the OUT stations and increased slightly, but within measurement error, between 50 and 125 m (Fig. 7F).

Discussion

Comparison of export flux to SOFeX carbon budget—We can use estimates of changes in C stock as an independent check on the magnitude of the POC export predicted here with the ^{234}Th approach. Coale et al. (2004) looked at measurements of total CO_2, POC, and gas exchange to determine a net decrease in C stocks in the South Patch mixed layer of 7 ± 7 μmol L^{-1}, equivalent to a flux of 12 mmol C m^{-2} d^{-1} when averaged over 50 m and 30 d. Corrections for patch dilution were not made, which would increase these geochemical signals by a factor of three. As seen in the large uncertainty on this C budget, it is difficult to quantify small changes in C loss from the depletion of much larger inorganic C stocks and build up of organic C pools. Not included in the Coale et al. (2004) C balance are changes in the DOC pool, so this change in C stocks could be accounted for either by POC export or DOC build-up. Our average 50-m POC flux IN and integrated over the same 30 d would average 7 mmol m^{-2} d^{-1} (Table 2). Thus, both estimates are in agreement, but the comparison is not rigorous.

Magnitude of SOFeX fluxes and comparisons to the Antarctic Ecosystem Southern Ocean Process Study—Despite enhanced fluxes of POC and $bSiO_2$ in response to Fe fertilization during SOFeX, the magnitude of these fluxes was not particularly large relative to the natural cycle of C uptake and export at this site. For example, in this same region and season in 1998 (U.S. Joint Global Ocean Flux Study, Antarctic Ecosystem Southern Ocean Process Stud [AESOPS]), we measured significantly lower ^{234}Th activities and higher associated particulate ^{234}Th, POC, and $bSiO_2$ fluxes, even when compared with the fertilized patch after 28 d (Table 3). The AESOPS POC fluxes were 5–10 times greater than the SOFeX OUT stations, and the final SOFeX IN POC flux was only half that observed in 1998. Also, there were five times greater $bSiO_2$ fluxes in February 1998 ($bSiO_2$: C export ratio = 0.33) than at the end of SOFeX IN (Table 3).

It is likely that the lower export fluxes and lower $bSiO_2$: C export ratios during SOFeX relative to AESOPS reflect a lower abundance of diatoms both in the ambient waters and in the plankton assemblage arising in response to Fe. This is supported by the significantly lower $bSiO_2$ concentrations measured during SOFeX compared with February 1998 (Table 3). The physical settings were different as well. The AESOPS stations had similar salinities and a somewhat shallower mixed layer in January, but AESOPS temperatures were about 1°C warmer within the mixed layer, and the mid-January biomass and primary production levels were much higher than equivalent SOFeX OUT stations. Thus, the biogeochemical conditions were different at the start of SOFeX, which might explain the low export fluxes (colder waters, lower diatom abundances). This comparison also points to the difficulty in characterizing Southern Ocean biogeochemistry, when even within a relatively well-studied region—in this case, south of the Antarctic Circumpolar Current Front

within the seasonal ice zone and in permanently high dissolved Si and N waters—considerable interannual variability in production and export fluxes can occur.

With respect to the SOFeX fluxes, it is important to note that the effects of iron addition very likely continued beyond the occupation of our last station. On day 28, surface waters were still Fe replete relative to phytoplankton growth requirements, such that biomass, photosynthetic efficiency, and other indicators suggested that the bloom had not ended (Coale et al. 2004). During AESOPS, a lag time of 2 weeks to >1 month was observed between the onset and termination of the bloom (Abbott et al. 2000; Buesseler et al. 2003). Here, Fe was added four times through day 12 in a deliberate attempt to keep the bloom from becoming Fe limited. Thus, our observation period was not likely long enough to see the onset of Fe limitation or other factors that might cause the termination of the SOFeX bloom.

Rates of C and Si export compared with production—Prior studies of Southern Ocean biogeochemistry suggest particularly high rates of export on sinking particles relative to primary production or $bSiO_2$ uptake south of the Antarctic Polar Front (Buesseler et al. 2001*b*, 2003). During SOFeX, the efficiency of POC and $bSiO_2$ export, defined as the ratio of export to production, was calculated for weeks 1, 2, and 3 with the use of all available data integrated over the upper 50 m. Although primary production, Si uptake, and POC export all increased during SOFeX in response to Fe, the export efficiency of organic carbon was significantly different from $bSiO_2$. Both tended to be higher at OUT stations compared with IN stations, but the differences were generally insignificant for $bSiO_2$. For C export efficiency, the lower fraction of C lost on sinking particles IN might be tied to Fe-replete conditions favoring more efficient retention of POC in response to the Fe-induced diatom bloom (*see next paragraph*).

Relative to each other, the efficiency of POC export was higher than that for biogenic silica both IN and OUT (above the 1 : 1 line in Fig. 10), with the ratio of POC : $bSiO_2$ export efficiency varying between 1.3 and 2.4. If the source of exported POC was entirely diatoms, then the greater efficiency of POC export compared with that of $bSiO_2$ would imply that $bSiO_2$ was more effectively recycled in the upper 50 m than was organic matter. This is unlikely because the turnover of organic matter is typically more rapid than that of $bSiO_2$ in surface waters. A more plausible explanation is that nonsiliceous plankton were preferentially being exported over diatoms both IN and OUT of the patch. This was unexpected because diatoms dominated the increase in phytoplankton biomass within the patch (Coale et al. 2004). Export of this bloom would yield the same export efficiency for carbon and silica in the patch. That this did not occur argues that the Fe-induced diatom bloom was not a dominant component of carbon export during the time frame of our experiment. Efficient retention of the diatom bloom in the surface waters is consistent with improved buoyancy control that would arise after release from Fe stress. Improved buoyancy control is observed under nutrient-replete conditions for many phytoplankton (Smayda 1970; Bienfang et al. 1982), but in this case, the diatoms were the major benefactors of the release from Fe stress. Whatever the mechanism retaining the bloom in surface waters, a large potential for carbon export by diatoms was unrealized within the time frame of our experiment.

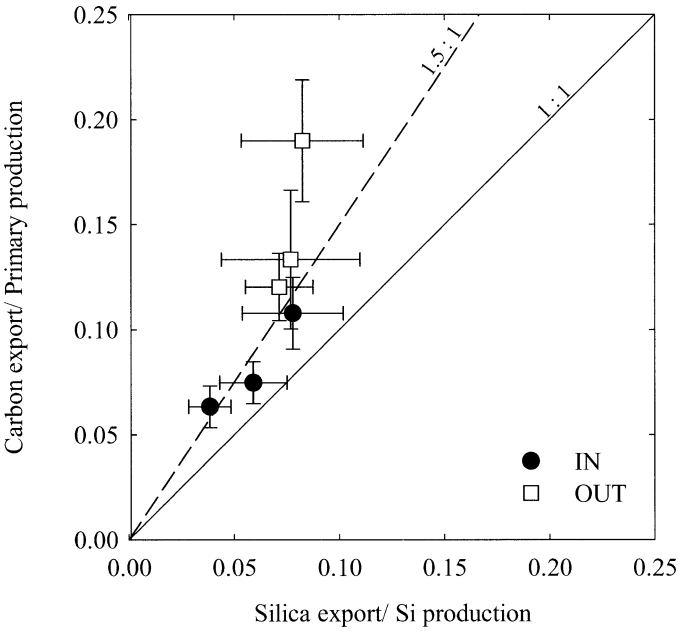

Fig. 10. The export efficiency of POC versus biogenic silica at IN (filled circles) and OUT stations (open squares). Rates of primary production and silica production were integrated to 50 m, and weekly averages were computed for each of the first 3 weeks following the initial Fe fertilization (data from R. Barber, V. Lance, and M. Brzezinski). Each weekly averaged, integrated production rate was then compared with the average rate of export at 50 m for the same time period (Table 2). Fifty meters was chosen as the depth best representative of the mixed layer, the approximate extent of Fe enrichment in the IN water column, which was about the 10% light depth. Lines drawn represent ratios of carbon : silica export efficiencies of 1 : 1 (solid line) and 1.5 : 1 (dashed line). Errors were determined from the standard error on the weekly export efficiency ratio (data are averages from n = 40, 11, and 10 stations for primary production, $bSiO_2$ uptake, and POC or bSi export, respectively).

Comparison with other Southern Ocean Fe studies—Only three other Southern Ocean iron fertilization experiments have been done to date with which we can compare the SOFeX South Patch: the Southern Ocean Iron Enrichment Experiment (SOIREE), the Eisen (= Iron) Experiment (EisenEx-1), and the North Patch of SOFeX. All three produced notable increases in biomass and associated decreases in dissolved inorganic carbon and associated nutrients (Boyd et al. 2000; Smetacek 2001; Bishop et al. 2004; Coale et al. 2004). SOIREE was initiated in February 1999 at 60°S, 140°E (Boyd et al. 2000), and during a 13-d observation period, the $^{234}Th : ^{238}U$ ratio increased similarly at both IN and OUT stations. The slope of the increase was explained by the natural ingrowth of ^{234}Th from ^{238}U during conditions of near zero net particle flux (Charette and Buesseler 2000). The ^{234}Th results agreed with the lack of clear IN compared with OUT differences in shallow sediment trap flux (Nodder et al. 2001) and with the satellite observation of the persis-

tence of the SOIREE patch 55 d after the beginning of the experiment (Abraham et al. 2000). Also, a comprehensive carbon balance for SOIREE did not reveal a significant carbon deficit that would indicate POC export (Bakker et al. 2001).

The pre-Fe release condition during EisenEx differed from SOIREE and SOFeX in that, at the start of observations (November 2000; 48°S, 21°E), there were no measurable ^{234}Th disequilibria (^{234}Th = ^{238}U; M. Rutgers van der Loeff pers. comm.). These data indicate the absence of significant particle export before arrival; therefore, EisenEx began before the start of the natural flux cycle. Indeed, as the 22-d experiment progressed, ^{234}Th activities decreased, indicating particle export, but IN and OUT stations were not different (U. Riebesell and M. M. Rutgers van der Loeff pers. comm.). Thus, on the basis of the ^{234}Th data alone, it does not appear as if there was Fe-enhanced particle export relative to the natural phytoplankton dynamics.

Somewhat at odds with the EisenEx ^{234}Th data were attempts to balance carbon stocks. On the basis of differences in the dissolved inorganic C and POC stocks alone, Riebessel et al. (pers. comm.) concluded that export IN was greater than OUT by 1,000 mmol C m^{-2} or 48 mmol C m^{-2} d^{-1} for the upper 80 m. As with SOFeX, it is very clear that biomass responded to Fe, but an exact accounting for export by looking at the difference in C stocks is difficult to constrain, in part because of the lack of DOC data.

The SOFeX North Patch (January–February 2002; 56°S, 172°W) attained roughly twice the primary production rates but lower Chl *a* levels than in the South patch after a similar series of Fe additions (Coale et al. 2004). Ship-based observations were limited to early and late conditions for the North Patch, but on the basis of data from an autonomous profiling float that measured particle abundances continuously, Bishop et al. (2004) concluded that POC flux increased significantly during a period 25–45 d after the first Fe addition. Using a POC flux calibration from a similar float in the South Patch, they estimate a POC flux of 2.4–23 mmol C m^{-2} d^{-1} at 100 m when averaged over the entire 50-d period. They favor the upper range of these POC flux estimates, and assuming this flux calibration is correct, the POC fluxes would be significantly higher than the 7 mmol C m^{-2} d^{-1} we observed on average during the first 28 d of the South Patch.

Coale et al. (2004) estimated C balance for the North Patch, by methods similar to those employed for the South Patch, equivalent to 8 mmol C m^{-2} d^{-1} (both after 28–30 d). However, because of limited sampling in the North Patch and a lack of data for some of the major C reservoirs, in particular dissolved organic carbon, the errors on these C balances are large. Bishop et al. (2004) speculated that the export response in the North Patch was triggered by a subduction of POC from a change in stratification that isolated the iron-stimulated biomass in a layer with reduced light and lower turbulence; however, the lack of concomitant biogeochemical data makes it impossible to rule out other causes. A similar subduction event was not observed in the South Patch.

We observed changes in the distribution of the particle-reactive radionuclide ^{234}Th in response to Fe addition in HNLC waters of the Southern Ocean. The Lagrangian sampling of SF_6-tagged waters allowed for an ideal application of this tracer; we could follow the evolving ^{234}Th activity distribution and quantify horizontal and vertical exchange processes to resolve small changes in ^{234}Th fluxes. The main feature is a decrease in ^{234}Th activity within the mixed layer attributable to enhanced particle export in response to iron.

We also saw a decrease in excess ^{234}Th below the Fe-fertilized patch, which indicated decreased particle remineralization beneath the patch. This implies that the particles leaving the upper ocean are more robust (less labile or sinking more rapidly), that the biological and physical processes responsible for particle degradation and break-up below the mixed layer have become less efficient, or a combination of both conditions. This subsurface response is not currently considered in our understanding of the possible biogeochemical effects of Fe in the ocean.

When converted to POC and $bSiO_2$ export rates, these fluxes were not large relative to natural blooms and were, in fact, smaller than those observed under natural conditions at this site during a different field season. The lack of a large SOFeX export response is consistent with models suggesting that for patches at scales of 10–100 km, natural dilution effects would reduce cell numbers, and thus limit aggregation, and hence the export response (Boyd et al. 2002). We can only speculate as to the ultimate fate of C in the SOFeX South Patch because no further ship observations or satellite images were obtained after the first month.

Ultimately, it is the sequestration of C and associated elements to the deep ocean that has the potential to influence climate as put forward by the iron hypothesis. Unfortunately, C flux to the deep ocean is difficult to assess. Ideally, one would quantify not just what leaves the Fe-fertilized patch, but the subsurface effects as well, such as seen here in the remineralization patterns of sinking particles and controls thereof. Mass balance approaches to quantify surface ocean C losses are inherently difficult because of the dynamic nature of patch dilution and the efforts needed to quantify in four dimensions all inorganic and organic C forms and exchanges, especially when the export fluxes are much smaller than standing stocks. Part of this difficulty is overcome with the use of ^{234}Th as an in situ tracer; transport terms are small relative to the radioactive production and decay rates, which are quantified by the ^{234}Th : ^{238}U disequilibrium, and dominate the thorium export flux calculation.

Many questions remain concerning the longer term fate of iron-induced blooms, including what factors trigger bloom termination and what fraction of the C taken up during photosynthesis would reach deeper waters that are not regularly ventilated. To better examine these questions, we must design experiments that stimulate substantial biomass increase, as well as terminate Fe addition early enough in the experiment so that we can observe the return of Fe limitation. Measurement of the export of multiple elements provides a means to assess the export contribution of different phytoplankton groups. The comparison of flux to rates of production yields insights into relative recycling rates of organic and inorganic constituents. Also, dilution effects need to be considered not just in the mass balance of major ele-

ments, but in the dynamics of aggregation. Larger patch scales might enhance aggregation and provide conditions more like the large-scale changes attributed to shifts in dust-born Fe input associated with glacial and interglacial cycles.

Thus far, few data have been collected on POC export in response to Fe. This study is one of the most complete and suggests relatively modest export response and low efficiency of C export relative to Fe added (Buesseler and Boyd 2003). The assumption that Fe addition would lead directly to large export has proven difficult to demonstrate. Studies to date even outside of the Southern Ocean are not convincing in demonstrating a large export response. There are limitations with different methods and difficulties in constraining C stocks and fluxes over perhaps too short an observation period. However, what has been found in the Southern Ocean supports a response that includes efficient recycling of Fe and observations of ecosystems that maintain high photosynthetic efficiency and chlorophyll biomass many weeks after Fe addition. This was demonstrated most dramatically by the satellite observations in SOIREE of the surface Chl *a* feature almost 2 months after Fe addition (Abraham et al. 2000). Therefore, the question remains open as to how the response to Fe, as seen in enhanced phytoplankton growth in HNLC regions, can be extrapolated to export and how this might change under different conditions. Certainly, geoengineering proposals to fertilize the ocean that claim to reduce build-up of greenhouse CO_2 via C sequestration in the deep ocean are not supported directly. However, because past changes in atmospheric CO_2 and climate have been correlated tightly to dust, and hence Fe sources to the ocean (Martin 1990), the issue of the ocean C flux response to iron and the fate of this sinking C remains an important question to resolve.

References

ABBOTT, M. R., J. G. RICHMAN, R. M. LETELIER, AND J. S. BARTLETT. 2000. The spring bloom in the Antarctic Polar Frontal Zone as observed from a mesoscale array of bio-optical sensors. Deep-Sea Res. II **47:** 3285–3314.

ABRAHAM, E. R., C. S. LAW, P. W. BOYD, S. J. LAVENDER, M. T. MALDONADO, AND A. R. BOWIE. 2000. Importance of stirring in the development of an iron-fertilized phytoplankton bloom. Nature **407:** 727–730.

BAKKER, D. C. E., A. J. WATSON, AND C. S. LAW. 2001. Southern Ocean iron enrichment promotes inorganic carbon drawdown. Deep-Sea Res. II **48:** 2483–2508.

BARBER, R. T., AND OTHERS. 1996. Primary productivity and its regulation in the equatorial Pacific during and following the 1991–1992 El Nino. Deep-Sea Res. II **43:** 933–969.

BENITEZ-NELSON, C., K. O. BUESSELER, AND G. CROSSIN. 2000. Upper ocean carbon export, horizontal transport, and vertical eddy diffusivity in the southwestern Gulf of Maine. Cont. Shelf Res. **20:** 707–736.

———, AND M. A. CHARETTE. 2004. Uncertainty versus variability in upper ocean carbon flux estimates. Limnol. Oceanogr. **49:** 1218–1220.

———, AND OTHERS. 2001. Testing a new small-volume technique for determining thorium-234 in seawater. J. Radioanal. Nucl. Chem. **248:** 795–799.

BIDIGARE, R. R., AND OTHERS. 1999. Iron-stimulated changes in ^{13}C fractionation and export by equatorial Pacific phytoplankton: Toward a paleogrowth rate proxy. Paleoceanography **14:** 589–595.

BIENFANG, P. K., P. J. HARRISON, AND L. M. QUARMBY. 1982. Sinking rate response to depletion of nitrate, phosphate and silicate in four marine diatoms. Mar. Biol. **67:** 295–302.

BISHOP, J. K. B., T. J. WOOD, R. E. DAVIS, AND J. T. SHERMAN. 2004. Robotic observations of enhanced carbon biomass and export at 55S during SOFeX. Science **304:** 417–420.

BOWIE, A. R., AND OTHERS. 2001. The fate of added iron during a mesoscale fertilisation experiment in the Southern Ocean. Deep-Sea Res. II **48:** 2703–2743.

BOYD, P. W., AND E. R. ABRAHAM. 2001. Iron-mediated changes in phytoplankton photosynthetic competence during SOIREE. Deep-Sea Res. II **48:** 2529–2550.

———, G. A. JACKSON, AND A. M. WAITE. 2002. Are mesoscale perturbation experiments in polar waters prone to physical artefacts? Evidence from algal aggregation modelling studies. Geophys. Res. Lett. **29:** 10.1029/2001GL014210.

———, AND OTHERS. 2000. A mesoscale phytoplankton bloom in the polar Southern Ocean stimulated by iron fertilization. Nature **407:** 695–702.

BRZEZINSKI, M. A., D. M. NELSON, V. M. FRANCK, AND D. E. SIGMON. 2001. Silicon dynamics within an intense open-ocean diatom bloom in the Pacific sector of the Southern Ocean. Deep-Sea Res. II **48:** 3997–4018.

BUESSELER, K. O. 1998. The decoupling of production and particulate export in the surface ocean. Glob. Biogechem. Cycles **12:** 297–310.

———, J. A. ANDREWS, M. C. HARTMAN, R. BELASTOCK, AND F. CHAI. 1995. Regional estimates of the export flux of particulate organic carbon derived from thorium-234 during the JGOFS EQPAC program. Deep-Sea Res. II **42:** 777–804.

———, ———, S. M. PIKE, AND M. A. CHARETTE. 2004. The effects of iron fertilization on carbon sequestration in the Southern Ocean. Science **304:** 414–417.

———, M. P. BACON, J. K. COCHRAN, AND H. D. LIVINGSTON. 1992. Carbon and nitrogen export during the JGOFS North Atlantic Bloom Experiment estimated from $^{234}Th:^{238}U$ disequilibria. Deep-Sea Res. I **39:** 1115–1137.

———, R. T. BARBER, M.-L. DICKSON, M. R. HISCOCK, J. K. MOORE, AND R. SAMBROTTO. 2003. The effect of marginal ice-edge dynamics on production and export in the Southern Ocean along 170°W. Deep-Sea Res. II **50:** 579–603.

———, AND P. W. BOYD. 2003. Will ocean fertilization work? Science **300:** 67–68.

———, AND OTHERS. 1998. Upper ocean export of particulate organic carbon in the Arabian Sea derived from thorium-234. Deep-Sea Res. II **45:** 2461–2487.

———, AND OTHERS. 2001*a*. An intercomparison of small- and large-volume techniques for thorium-234 in seawater. Mar. Chem. **74:** 15–28.

———, AND OTHERS. 2001*b*. Upper ocean export of particulate organic carbon and biogenic silica in the Southern Ocean along 170°W. Deep-Sea Res. II **48:** 4275–4297.

CHARETTE, M. A., AND K. O. BUESSELER. 2000. Does iron fertilization lead to rapid carbon export in the Southern Ocean? Geochemistry, Geophysics, Geosystems paper no. 2000GC000069.

———, S. B. MORAN, S. M. PIKE, AND J. N. SMITH. 2001. Investigating the carbon cycle in the Gulf of Maine using the natural tracer thorium-234. J. Geophys. Res., C **106:** 11553–11579.

CHEN, J. H., R. L. EDWARDS, AND G. J. WASSERBURG. 1986. ^{238}U, ^{234}U and ^{232}Th in seawater. Earth Planet. Sci. Lett. **80:** 241–251.

COALE, K. H., K. S. JOHNSON, S. E. FITZWATER, S. P. G. BLAIN, T. P. STANTON, AND T. L. COLEY. 1998. Iron Ex-I, an in situ iron-

enrichment experiment: Experimental design, implementation and results. Deep-Sea Res. II **45:** 919–946.

———, AND OTHERS. 1996. A massive phytoplankton bloom induced by an ecosystem-scale iron fertilization experiment in the equatorial Pacific Ocean. Nature **383:** 495–501.

———, AND OTHERS. 2004. Southern Ocean iron enrichment experiments (SOFeX) expand extent of iron limitation and carbon flux in Southern Ocean. Science **304:** 408–413.

COCHRAN, J. K., K. A. ROBERTS, C. BARNES, AND D. ACHMAN. 1997. Radionuclides as indicators of particle and carbon dynamics on the East Greenland Shelf, p. 129–136. *In* J.C.G.P. Germain, P. Guegueniat, and H. Metivier [eds.], RADOC 96–97 ''Radionuclides in the Oceans.'' Radioprotection-colloques, 32(C2). Les Éditions de Physique.

DUNNE, J. P., AND J. W. MURRAY. 1999. Sensitivity of ^{234}Th export to physical processes in the central equatorial Pacific. Deep Sea Res. I **46:** 831–854.

GARDNER, W. D., M. J. RICHARDSON, C. A. CARLSON, D. A. HANSELL, AND A. V. MISHONOV. 2003. Determining true particulate organic carbon: Bottles, pumps and methodologies. Deep-Sea Res. II **50:** 655–692.

GOLDSON, L. E. 2004. Vertical mixing across the seasonal pycnocline in the Southern Ocean: Studies using SF6 tracer. Ph.D. thesis, University of East Anglia, U.K.

GUSTAFSSON, Ö., K. O. BUESSELER, W. R. GEYER, S. B. MORAN, AND P. M. GSCHWEND. 1998. On the relative significance of horizontal and vertical transport of chemicals in the coastal ocean: Application of a two-dimensional Th-234 cycling model. Cont. Shelf Res. **18:** 805–829.

HOLM-HANSEN, O., C. J. LORENZEN, R. W. HOLMES, AND J. D. H. STRICKLAND. 1965. Fluorometric determination of chlorophyll. J. Cons. **30:** 3–15.

HUNTER, C. N., R. M. GORDON, S. E. FITZWATER, AND K. H. COALE. 1996. A rosette system for the collection of trace metal clean seawater. Limnol. Oceanogr. **41:** 1367–1372.

HUNTSMAN, S. A., AND R. T. BARBER. 1977. Primary production off northwest Africa: The relationship to wind and nutrient conditions. Deep-Sea Res. **24:** 25–33.

LORENZEN, C. J. 1966. A method for the continuous measurement of in vivo chlorophyll concentration. Deep-Sea Res. **13:** 223–227.

MARTIN, J. H. 1990. Glacial-interglacial CO_2 change: The iron hypothesis. Paleoceanography **5:** 1–13.

MORAN, S. B., M. A. CHARETTE, S. M. PIKE, AND C. A. WICKLUND. 1999. Differences in seawater particulate organic carbon concentration in samples collected using small-volume and large-volume methods: The importance of DOC adsorption to the filter blank. Mar. Chem. **67:** 33–42.

———, AND OTHERS. 2003. Does ^{234}Th/^{238}U disequilibrium provide an accurate record of the export flux of particulate organic carbon from the upper ocean? Limnol. Oceanogr. **48:** 1018–1029.

MORRISON, J. M., AND OTHERS. 2001. Seasonal evolution of hydrographic properties in the Antarctic Circumpolar Current at 170°W during 1997–1998. Deep-Sea Res. II **48:** 3943–3972.

NODDER, S. D., AND OTHERS. 2001. Particle transformations and export flux during an in situ iron-stimulated algal bloom in the Southern Ocean. Geophys. Res. Lett. **28:** 2409–2412.

PIKE, S., K. O. BUESSELER, J. A. ANDREWS, AND N. SAVOYE. In press. Quantification of 234Th recovery in small volume sea water samples by inductively coupled plasma mass spectrometry. J. Radioanal. Nucl. Chem.

———, AND S. B. MORAN. 1997. Use of Poretics 0.7 μm pore size glass fiber filters for determination of particulate organic carbon and nitrogen in seawater and freshwater. Mar. Chem. **57:** 355–360.

SANTSCHI, P. H., AND OTHERS. 2003. Control of acid polysaccharide production and ^{234}Th and POC export fluxes by marine organisms. Geophys. Res. Lett. **30:** 1044, doi:1010.1029/2002GL016046.

SMAYDA, T. J. 1970. The suspension and sinking of phytoplankton in the sea. Oceanogr. Mar. Biol. Annu. Rev. **8:** 353–414.

SMETACEK, V. S. 2001. EisenEx: International team conducts iron experiments in Southern Ocean. U.S. JGOFS Newsl. **11:** 11–14.

TSUNOGAI, S., K. TAGUCHI, AND K. HARADA. 1986. Seasonal variation in the difference between observed and calculated particulate fluxes of Th-234 in Funka Bay, Japan. J. Oceanogr. Soc. Jpn. **42:** 91–98.

VENRICK, E. L., AND T. L. HAYWARD. 1984. Determining chlorophyll on the 1984 CalCOFI surveys. Calif. Coop. Ocean. Fish. Invest. Rep. **25:** 74–79.

WATSON, A. J., P. J. LISS, AND R. A. DUCE. 1991. Design of a small-scale in situ iron fertilization experiment. Limnol. Oceanogr. **36:** 1960–1965.

WEI, C.-L., AND J. W. MURRAY. 1992. Temporal variations of ^{234}Th activity in the water column of Dabob Bay: Particle scavenging. Limnol. Oceanogr. **37:** 296–314.

Received: 2 February 2004
Accepted: 11 July 2004
Amended: 29 July 2004